

Drosomycin, an Innate Immunity Peptide of *Drosophila melanogaster*, Interacts with the Fly Voltage-gated Sodium Channel*

Received for publication, May 20, 2009, and in revised form, June 27, 2009. Published, JBC Papers in Press, July 1, 2009, DOI 10.1074/jbc.M109.023358

Lior Cohen^{#1,2,3}, Yehu Moran^{#1}, Amir Sharon[#], Daniel Segal[§], Dalia Gordon[#], and Michael Gurevitz^{#4}

From the Departments of [#]Plant Sciences and [§]Molecular Microbiology and Biotechnology, George S. Wise Faculty of Life Sciences, Tel Aviv University, Ramat Aviv, 69978 Tel Aviv, Israel

Several peptide families, including insect antimicrobial peptides, plant protease inhibitors, and ion channel gating modifiers, as well as blockers from scorpions, bear a common CS α β scaffold. The high structural similarity between two peptides containing this scaffold, drosomycin and a truncated scorpion β -toxin, has prompted us to examine and compare their biological effects. Drosomycin is the most expressed antimicrobial peptide in *Drosophila melanogaster* immune response. A truncated scorpion β -toxin is capable of binding and inducing conformational alteration of voltage-gated sodium channels. Here, we show that both peptides (i) exhibit anti-fungal activity at micromolar concentrations; (ii) enhance allosterically at nanomolar concentration the activity of Lqh α IT, a scorpion alpha toxin that modulates the inactivation of the *D. melanogaster* voltage-gated sodium channel (DmNa_v1); and (iii) inhibit the facilitating effect of the polyether brevetoxin-2 on DmNa_v1 activation. Thus, the short CS α β scaffold of drosomycin and the truncated scorpion toxin can maintain more than one bioactivity, and, in light of this new observation, we suggest that the biological role of peptides bearing this scaffold should be carefully examined. As for drosomycin, we discuss the intriguing possibility that it has additional functions in the fly, as implied by its tight interaction with DmNa_v1.

The cysteine-stabilized $\alpha\beta$ scaffold, CS α β , contains an α -helix packed against a two-stranded β -sheet stabilized by three spatially conserved disulfide bonds (reviewed in Ref. 1). The CS α β motif appears in a number of polypeptide families that can exert various biological functions such as: short chain (30–50 residues long) and long chain (60–76 residues long) scorpion toxins that affect voltage-gated ion channels, antimi-

crobial peptides (of insect and plants) as well as plant protease inhibitors (see Fig. 1) (2, 3).

Analysis of the structure-function relationships of several representatives of a subclass of the long chain scorpion toxins family, the scorpion β -toxins (activators of voltage-gated sodium channels (Na_vs)⁵), elucidated their bioactive surfaces including those of the anti-insect excitatory and depressant toxins Bj-xtrIT and LqhIT2 (from *Hottentota judaica* and *Leiurus quinquestriatus hebraeus*, respectively (4–6)) and the anti-mammalian β -toxin C β s4 (from *Centruroides suffusus suffusus* (7)). These studies highlighted a conserved pharmacophore positioned on the CS α β protein core (7). The C-tail, loops, turns, and unstructured stretches that connect to the CS α β protein core in long chain scorpion toxins constitute a large portion of their exteriors and bear residues that participate in bioactivity (reviewed in Ref. 8). We have recently reported that truncated scorpion β -toxins, lacking the N- and C-terminal regions of the parental peptides but maintaining the CS α β motif ($\Delta\Delta\beta$ -toxins), are able to interact at high affinity with Na_vs (9). Although by themselves, the $\Delta\Delta\beta$ -toxins ($\Delta\Delta$ C β s4 and $\Delta\Delta$ Bj-xtrIT) were nontoxic and did not bind at the receptor sites of the parental toxins, they exhibited an unexpected ability to allosterically facilitate the activity of a scorpion α -toxin (inhibition of Na_v fast inactivation), which binds at receptor site-3 on insect Na_vs (10), and the effect of the marine polyether toxin brevetoxin-2 (PbTx-2, facilitator of Na_v activation), which binds to receptor site-5 (11). However, a short chain potassium channel blocker (charybdotoxin) with a CS α β structural fold did not exert any of these effects (9). These results indicated that it is not only the CS α β motif but that specific amino acids at key sites on the protein exterior that can interact with ion channels and either block voltage-gated potassium channels or induce conformational alteration of voltage-gated sodium channels. From a structural viewpoint, the ability of $\Delta\Delta$ Bj-xtrIT and $\Delta\Delta$ C β s4 to bind to the Na_v, as manifested in modulation of the interaction of receptor site-3 and -5 ligands, suggests that by truncation of the two β -toxins, a masked functional surface was exposed. Because the CS α β motif appears in several protein families including antimicrobial peptides, potassium channel blockers, and sodium channel gating modifiers (Fig. 1) (2, 3), we explored the possibility that a well characterized CS α β peptide

* This work was supported by the United States-Israel Binational Agricultural Research and Development Grants IS-3928-06 (to M. G. and D. G.) and IS-4066-07 (to D. G. and M. G.) and by Israeli Science Foundation Grants 1008/05 (to D. G. and M. G.) and 107/08 (to M. G. and D. G.).

¹ Both authors contributed equally to this work.

² Current address: Dept. of Neurobiology, Institute for Life Sciences, The Hebrew University of Jerusalem, Givat Ram, Jerusalem 91904, Israel.

³ To whom correspondence may be addressed: Dept. of Plant Sciences, George S. Wise Faculty of Life Sciences, Tel Aviv University, Ramat Aviv, Tel Aviv 69978, Israel. Tel.: 972-3-6409844; Fax: 972-3-6406100; E-mail: lcohen76@cc.huji.ac.il.

⁴ To whom correspondence may be addressed: Dept. of Plant Sciences, George S. Wise Faculty of Life Sciences, Tel Aviv University, Ramat Aviv, Tel Aviv 69978, Israel. Tel.: 972-3-6409844; Fax: 972-3-6406100; E-mail: mamgur@post.tau.ac.il.

⁵ The abbreviations used are: Na_v, voltage-gated sodium channel; DRS, drosomycin; $\Delta\Delta$ Bj-xtrIT, truncated *Hottentota judaica* excitatory toxin; $\Delta\Delta$ C β s4, truncated *Centruroides suffusus suffusus* toxin 4; DmNa_v1, *Drosophila melanogaster* voltage-gated sodium channel; PbTx-2, brevetoxin-2.

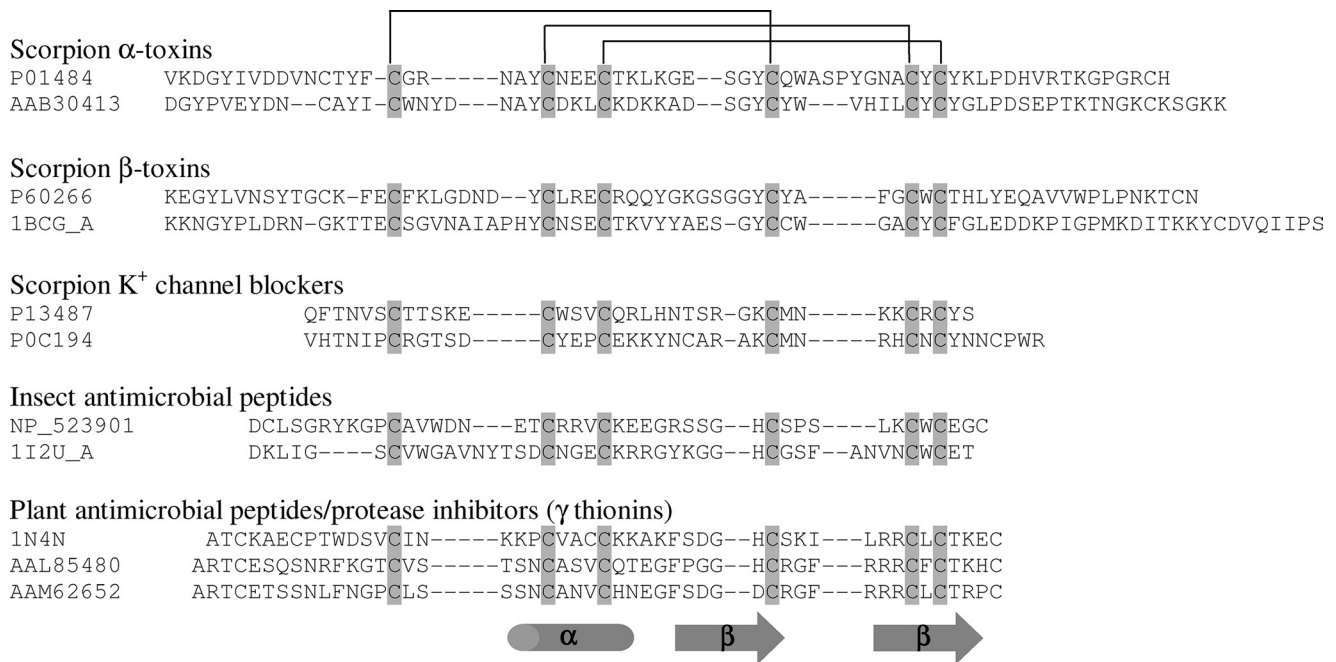


FIGURE 1. **Diversity of peptides containing the CS α β motif.** Representatives from each of five major groups of peptides containing a CS α β motif are aligned according to their conserved disulfide bridging and common structural features: two β -strands packed against an α -helix. The featured molecules are from a diverse array of organisms. Scorpion α -toxins: P01484 (Aah2 of the North African scorpion *Androctonus australis Hector*), AAB30413 (Ts4 of the Brazilian scorpion *Tityus serrulatus*); Scorpion β -toxins: P60266 (C α 4 of the Mexican scorpion *Centruroides suffusus suffusus*), 1BCG_A (Bj-xtrIT of the Israeli black scorpion *Hottentota judaica*); Scorpion potassium channel blockers: P13487 (charybdotoxin of the Israeli yellow scorpion *Leiurus quinquestriatus hebraeus*), P0C194 (α -KTx 6.11 of the scorpion *Opisthacanthus madagascariensis* of Madagascar); Insect antimicrobial peptides: NP_523901 (drosomycin of the fruit fly *Drosophila melanogaster*), 1I2U_A (heliomicin of the tobacco budworm *Heliothis virescens*); plant γ -thionins: 1N4N (defensin of the garden petunia *Petunia hybrida*), AAL85480 (defensin of peach *Prunus persica*), AAM62652 (protease inhibitor II of the thale cress *Arabidopsis thaliana*).

may exert an additional function known for other peptides bearing this scaffold.

For this aim, we tested the ability of a well characterized *Drosophila melanogaster* anti-fungal peptide drosomycin (DRS) to interact with voltage-gated sodium channels. The solution structure of DRS indicates that this 44-amino acid peptide is cross-linked by four disulfide bonds, of which three render a CS α β structural fold (Fig. 2) (12). Sequence comparison of the truncated scorpion β -toxin $\Delta\Delta$ C α 4 with DRS indicates moderate identity (34%) and similarity (50%), including conservation of six cysteine residues that stabilize the CS α β motif, which is manifested by a remarkable structural similarity (Fig. 2). Moreover, Lys-3, Asp-11, Asn-12, Glu-13, Gln-21, and Gln-22 of $\Delta\Delta$ C α 4, which are involved in the interaction with insect Na_vs, are spatially conserved in DRS (Fig. 2) (9) but not in potassium channel blockers (Fig. 1). In light of the resemblance between the truncated scorpion β -toxin and DRS, we tested whether DRS is able to interact with the *D. melanogaster* voltage-gated sodium channel DmNa_v1.

EXPERIMENTAL PROCEDURES

Neuropeptides—The expression and purification of DRS were carried out as described previously for a disulfide-bridged neurotoxin (13). Briefly, the sequence encoding the mature drosomycin was amplified via PCR from *D. melanogaster* genomic DNA and cloned into the NcoI and BamHI sites of a pET-32b expression vector derivative used for transformation of *Escherichia coli* strain Rosetta-gami (Novagen). The recombinant DRS, fused to thioredoxin and a His₆ tag, was purified on a HisTrap[®] affinity column (GE Healthcare), and

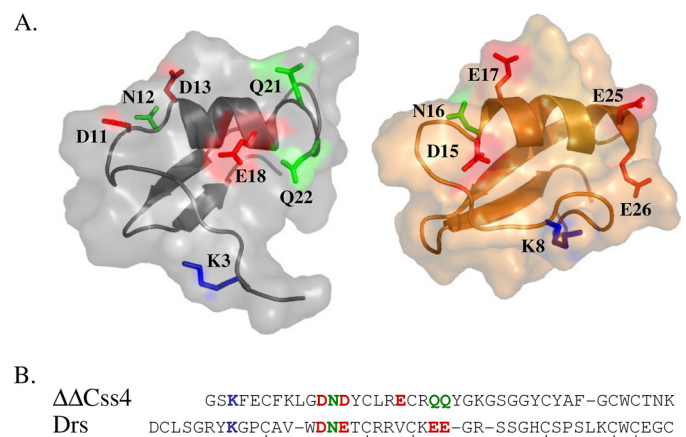


FIGURE 2. **Sequence alignment and three-dimensional structures of $\Delta\Delta$ C α 4 and DRS.** A, schematic diagrams of the C α model structures of $\Delta\Delta$ C α 4 and DRS covered by semitransparent molecular surfaces. The structure of DRS (right panel) is derived from the Protein Data Bank code 1MYN. The $\Delta\Delta$ C α 4 model (left panel) is based on the NMR structure of Cn2 (Protein Data Bank code 1Cn2) and is spatially aligned with that of DRS. A was prepared using PyMOL. B, sequences were aligned according to the conserved cysteine residues, and the disulfide bonds formed between cysteine pairs are marked in solid lines. Dashes indicate gaps. Amino acid residues that were identified as part of the interacting surface of $\Delta\Delta$ C α 4 with insect Na_vs (9) are shown in sticks according to their chemical nature (blue, positive charge; red, negative charge; green, nonpolar) and are also highlighted in the sequence alignment. Corresponding residues in DRS according to sequence and structural alignments are also shown in sticks.

the tag and thioredoxin were cleaved with thrombin. DRS was purified using a Resource[®] 3-ml reverse phase high pressure liquid chromatography column (GE Healthcare). The molecular mass of the recombinant DRS was confirmed by

Drosomycin Interaction with DmNa_v1

mass spectroscopy (predicted, 5,252.1 g/mol; measured, 5,251.9 g/mol).

The truncated scorpion β -toxins $\Delta\Delta$ Css4 and $\Delta\Delta$ Bj-xtrIT were produced as described previously (9). The scorpion α -toxin Lqh α IT was produced in recombinant form as was described previously (14). Brevetoxin 2 (PbTx-2) was purchased from Latoxan (Valence, France).

Antifungal Activity—*Botrytis cinerea* strain B05-10 was cultured on potato dextrose agar at 22 °C. *Colletotrichum gloeosporioides* forma specialis *aeschynomene* strain 3.1.3 was cultured on Emerson YpSs agar medium at 28 °C. Spores were collected from 7-day old (*B. cinerea*) or 5-day old (*C. gloeosporioides*) cultures by washing the plates with 5 ml of potato dextrose broth or regeneration medium, respectively. The spores were counted, diluted to a final concentration of 10⁵ spores/ml, and then dispensed into 48-well plates (0.5 ml/well). The plates were incubated under continuous light at 22 °C (*B. cinerea*) or 28 °C (*C. gloeosporioides*) with constant agitation at 150 rpm. The $\Delta\Delta\beta$ -toxins or DRS were added to the wells (in duplicate) from stock solutions, and the effect on growth was determined by measuring the absorbance at 600 nm after 24 and 48 h. The inhibition of growth was normalized to the growth without peptides. Heat-inactivated spores were used as a blank reference.

Toxicity Assays—Third instar *D. melanogaster* larvae (wild type Canton-S strain) were injected with 100 nl of toxin or toxins mixture by a pooled glass capillary mounted on a microdispenser under a $\times 40$ magnification. Four-day-old *Sarcophaga falculata* larvae (150 \pm 20 mg body weight) were injected intersegmentally with five to seven concentrations of each toxin or mixture of toxins (nine larvae in each group) in three independent experiments. ED₅₀ (effective dose) values for both species were calculated as was described previously (15). A positive result for Lqh α IT was scored when a characteristic contraction paralysis was observed 1–5 min postinjection. (Longer durations did not change the ED₅₀ values.) Lqh α IT and DRS were mixed at various ratios, and the ED₅₀ of each mixture was scored. When a mixture of a toxin and DRS was injected at doses close to its ED₅₀ value, the contraction paralysis developed at a slower rate, and, therefore, it was scored after 10–15 min.

Two-electrode Voltage Clamp Experiments—The cloned cDNA encoding for the *D. melanogaster* sodium channel α -subunit (DmNa_v1) and the auxiliary TipE subunit were kindly provided by J. Warmke, Merck, and M. S. Williamson, Division of Plant and Invertebrate Ecology-Rothamsted, UK, respectively. These cDNAs were transcribed *in vitro* using T7 RNA-polymerase and the mMACHINE™ system (Ambion, Austin, TX), and the cRNAs were injected into *Xenopus laevis* oocytes as was described (16). Currents were measured 1–2 days after injection using a two-electrode voltage clamp and a GeneClamp 500 amplifier (Axon Instruments, Union City, CA). Data were sampled at 10 kHz and filtered at 5 kHz. Data acquisition was controlled by a Macintosh PPC 7100/80 computer equipped with ITC-16 analog/digital converter (Instrutech Corp., Port Washington, NY), utilizing Synapse (Synergistic Systems). Capacitance transients and leak currents were removed by subtracting a scaled control trace

utilizing a P/6 protocol. Bath solution contained 96 mM NaCl, 2 mM KCl, 1 mM MgCl₂, 2 mM CaCl₂, and 5 mM HEPES, pH 7.85. Oocytes were washed with the bath solution using a BPS-8 perfusion system (ALA Scientific Instruments, Westbury, NY) with 4 p.s.i. positive pressure. Toxins were diluted with bath solution and applied directly to the bath to the final desired concentration.

RESULTS

To clarify whether the structural similarity between DRS and the truncated scorpion toxins is manifested at the functional level, we examined their antifungal and sodium channel activities. The recombinant DRS inhibited the growth of two fungal species, *B. cinerea* (~50% inhibition at 1.5 μ M) and *C. gloeosporioides* (~50% inhibition at 15 μ M), similar to the inhibition of fungal growth reported for the recombinant (17) and native DRS (isolated from flies after septic injury) (18). Notably, both $\Delta\Delta$ Css4 and $\Delta\Delta$ Bj-xtrIT also inhibited the growth of *C. gloeosporioides* (~50% inhibition at 15 μ M) but not the growth of *B. cinerea*. Different patterns of preference toward various species of fungi were previously reported for DRS and its homologues (17, 18).

Analysis of DRS at concentrations up to 5 μ M on DmNa_v1 expressed in *X. laevis* oocytes has shown no effect on the conductance and gating properties (Fig. 3). However, as we have recently demonstrated, the interaction of various peptides with Na_vs can be monitored indirectly by the allosteric effects imposed upon the activity of another channel ligand (9, 15). Using this sensitive assay, we examined whether the inhibitory effect of the scorpion α -toxin Lqh α IT (a site-3 Na_v ligand) on DmNa_v1 inactivation would be modulated by DRS. Lqh α IT increased the Na⁺ peak current and inhibited DmNa_v1 fast inactivation with an EC₅₀ of 2.6 \pm 0.2 nM (Fig. 4A) (9, 13). When Lqh α IT was applied together with DRS in a 1:50 molar ratio, the EC₅₀ of Lqh α IT in the context of the mixture dropped markedly to 0.9 \pm 0.2 nM (Fig. 4A). Analysis of the enhancement induced by DRS at a constant Lqh α IT concentration indicated facilitation of the α -toxin activity in a dose-dependent manner with an EC₅₀ of 56 \pm 11 nM (Fig. 4B). These data implied that DRS interacted with DmNa_v1, and, therefore, we examined its allosteric effect on the activity of PbTx-2 (a site-5 Na_v ligand). Whereas PbTx-2 at a concentration of 0.5 μ M shifted the voltage dependence of DmNa_v1 activation to more hyperpolarizing membrane potentials, pre- or co-application of PbTx-2 in a 1:2 molar ratio with DRS strongly suppressed this effect (Fig. 4C). Thus, the ability of DRS to allosterically modulate the activity of various Na_v ligands indicates that it binds to the sodium channel and induces a conformational alteration.

We further examined the interaction of DRS with the *D. melanogaster* Na_v *in vivo*. Lqh α IT, DRS, or a mixture of both were injected into third instar larvae, and the paralytic effects were monitored. Lqh α IT induced contraction paralysis of the larvae with half-maximal ED₅₀ of 35 pg/larva. The effect of Lqh α IT was strongly enhanced by co-injection with DRS (1:20 molar ratio), and the mixture ED₅₀ dropped ~4-fold to 8 pg/larva. It should be noted that DRS by itself induced weak symptoms of contraction paralysis in the larvae only at doses >5 ng/larva (>30-fold higher than those required for facilitation

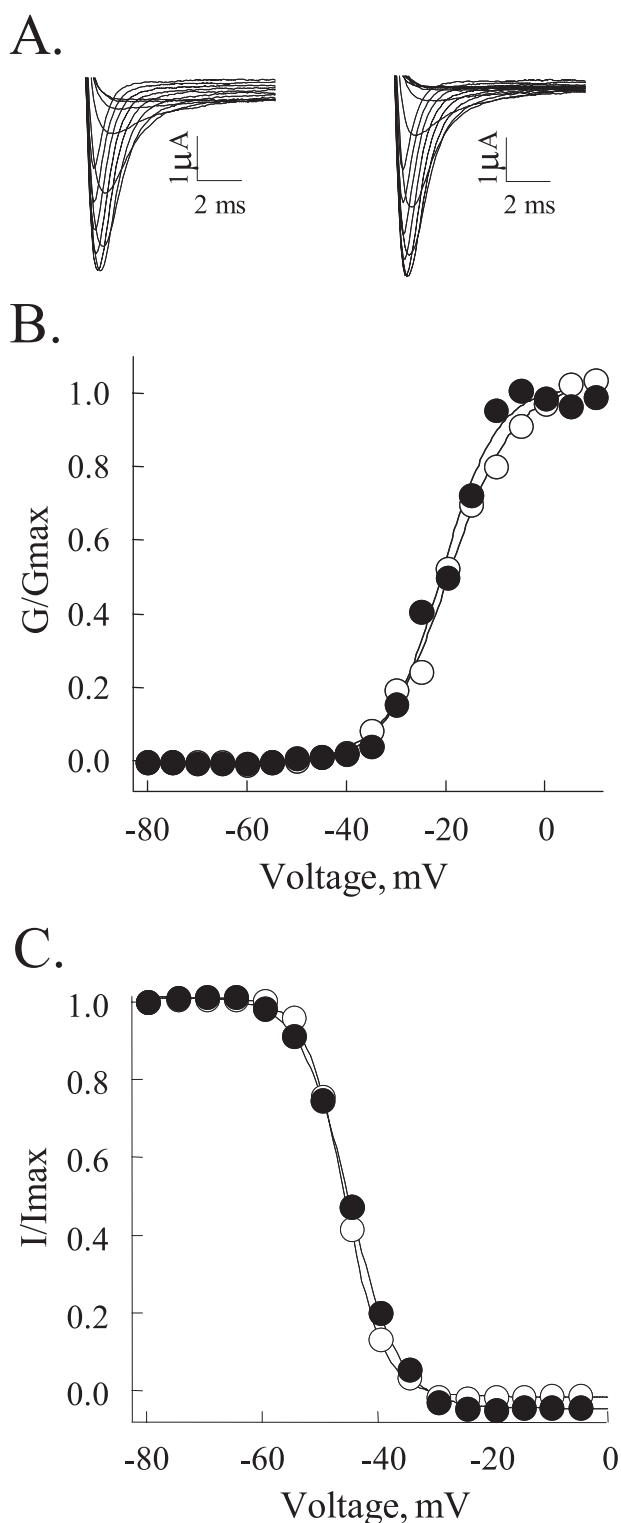


FIGURE 3. DRS has no effect on the gating properties of DmNa_v1. A, currents induced by a test pulse (50 ms) ranging from -80 to 0 mV (5 mV increments) of oocytes expressing DmNa_v1/TipE. Left panel, control; right panel, 5 μM DRS. B, conductance-voltage relationship of DmNa_v1 (open circles; V_{0.5} = -19.1 ± 0.5 mV, K = 5.5 ± 0.4), and in the presence of 5 μM DRS (black circles; V_{0.5} = -20.7 ± 0.7 mV, K = 5.5 ± 0.5). G/G_{max}, relative conductance. C, steady-state fast inactivation was determined from holding potential of -80 mV using a series of 50 ms prepulses from -80 to -0 mV in 5 mV increments prior to the test pulse (50 ms) to -10 mV. The steady-state inactivation of DmNa_v1 (open circles) fits a Boltzmann function with V_{0.5} = -45.6 ± 0.1 mV (k = 3.4 ± 0.1), and in the presence of 5 μM DRS (black circles) V_{0.5} = -44.7 ± 0.1 mV (k = 4.3 ± 0.1). I/I_{max}, relative current.

tion of LqhαIT activity). To better quantify this enhancing effect, toxicity assays were performed on the larger and more robust larvae of *S. falculata*. Although *S. falculata* belongs to a different fly superfamily, DRS increased by 6-fold the toxicity of LqhαIT toward these larvae in a dose-dependent manner, with an EC₅₀ of 14 ng/100 mg larvae (~30 nM, assuming that the weight of the larva equals its volume) (Fig. 5).

DISCUSSION

Here we show that a naturally occurring antifungal peptide with a structural scaffold common to toxins that target ion channels interacts with a voltage-gated sodium channel. Drosomycin enhances allosterically the activity of LqhαIT, a scorpion α-toxin that modulates the inactivation of the *D. melanogaster* voltage-gated sodium channel (DmNa_v1), and inhibits the facilitating effect on DmNa_v1 activation induced by the marine polyether brevetoxin-2 (Fig. 4). These results are highly similar to those obtained for the truncated β-toxins (9), probably due to the remarkable structure similarity as well as the spatial conservation of residues important for these activities in DRS and ΔΔC_{ss}4. This supports the hypothesis that drosomycin and scorpion toxins that affect ion channels, both harboring the CSαβ motif, might have evolved from a common progenitor (2, 3). Moreover, DRS, ΔΔC_{ss}4, and ΔΔBj-xtrIT induce both antifungal activity and allosteric conformational alteration of Na_vs. These intriguing results suggest that a peptide with a CSαβ scaffold can exert two different functions, and it seems that the chemical nature of the amino acid presented on this scaffold determines the peptide activities. Indeed, charybdotoxin, which adopts a CSαβ scaffold, lacks the ability to modulate Na_vs as the positions that enable the activity of ΔΔC_{ss}4 are not conserved in this potassium channel blocker (Fig. 1) (9). Because CSαβ peptides may support more than a single biological activity with different potencies, we suggest that the biological role of such peptides should be carefully reexamined to explore other potential functions that might have been overlooked.

The systemic antimicrobial response of *D. melanogaster* is triggered by pathogen infiltration through the cuticle, causing transient synthesis of antibacterial and antifungal peptides (19). Septic injury of *D. melanogaster* larvae or adults induces the transcription and translation of these peptides, of which DRS is the most prominent (18). The gene encoding DRS is a member in a family of seven homologous clustered loci (17, 20), of which the transcription of *Drs*, *dro3*, *dro4*, and *dro5* was demonstrated (21), and microarray analysis has shown that fungal infection of *D. melanogaster* leads to notable up-regulation of *Drs* and *dro5* transcription (22). Remarkably, DRS concentration in the fly hemolymph can reach 100 μM ~24 h postinfection (23, 24), probably to compensate for its relatively low antifungal potency (this work and Ref. 17). Still, despite the extensive documentation of its effect on fungi, the mechanism of action of DRS and its molecular targets are unknown at present.

The ability of DRS to interact with DmNa_v1 suggests that it might affect this channel as a result of pathogen infiltration, but the biological outcome of this interaction is yet to be determined. The sensitivity of available drosomycin-deficient strains such as *Drs* knock-out and knockdown or Toll receptor

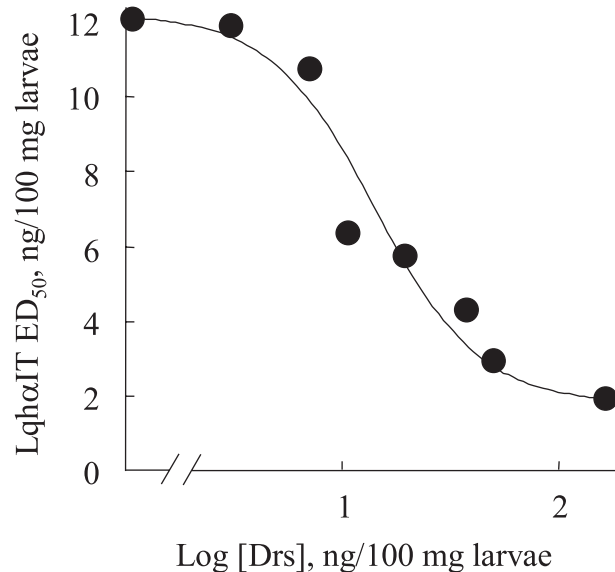
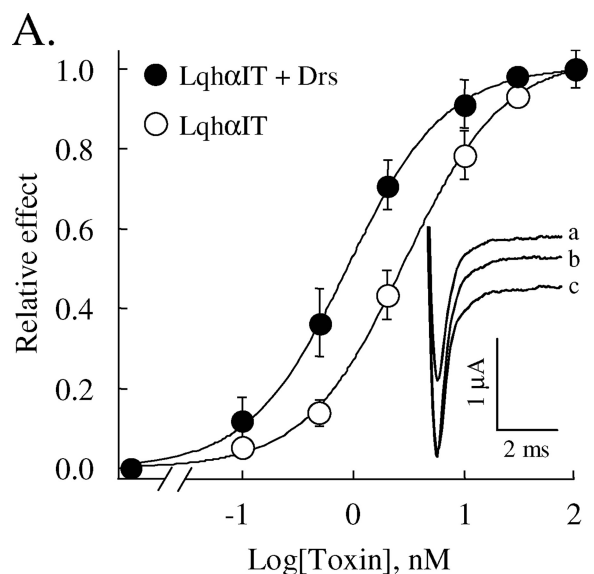
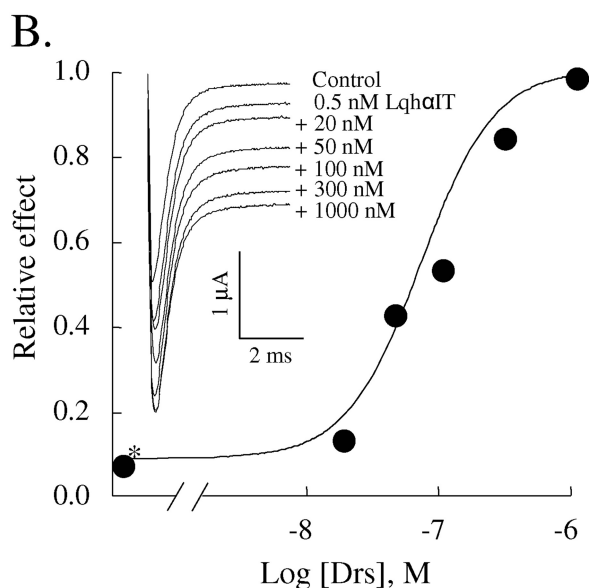


FIGURE 5. **Enhancement of LqhαIT toxicity by DRS.** Dose-response curve for toxicity of LqhαIT upon injection to *S. falculata* larvae in the presence of increasing concentrations of DRS. Forty larvae were used to generate each data point, which represents the ED₅₀ equivalent of LqhαIT in the presence of the indicated dose of DRS. The half-maximal dose of DRS (EC₅₀) that increases the toxicity (decrease in ED₅₀) of LqhαIT is 14 ng/100 mg larvae. Maximal enhancement in LqhαIT toxicity (~600%) is achieved in the presence of less than 200 ng of DRS.



(upstream regulator of drosomycin) knock-out strains, to LqhαIT injection will probably be similar to the sensitivity of wild type flies used in this study, as the expression of drosomycin is already very low in noninfected wild type strains (18). Therefore, such strains will not be effective in testing the *in vivo* existence and biological role of the suggested interaction between the native DRS and DmNa_v1. Ideally, a *Drosophila* strain that mimics specifically the response of the *Drs* locus to an immune challenge (exclusive overexpression of *Drs* under inducible conditions) may help answer these questions. However, as far as we are aware, only a constitutively expressing DRS strain has been reported thus far (25).

As DRS effect at the fly Na_v is observed at nM concentrations (Figs. 4 and 5), it is plausible that already at low concentrations

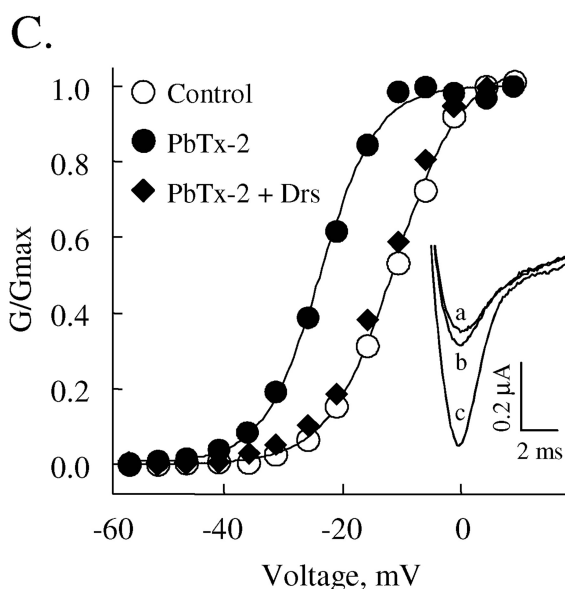


FIGURE 4. **Modulation of the effects of gating modifiers at DmNa_v1 by DRS.** Oocytes expressing DmNa_v1/TipE were clamped at -80 mV, and currents were elicited by step depolarizations of 50 ms to -10 mV. A, increasing concentrations of the toxin and toxin mixture with DRS were applied, and their relative effects on the current inactivation (sustained current) at -10 mV were determined after 50 ms. Activity of LqhαIT (empty symbols; EC₅₀ = 2.6 ± 0.2 nM; n = 4) and LqhαIT in a mixture with DRS (filled symbols; 1:50 molar ratio) on DmNa_v1 provided an EC₅₀ value of 0.9 ± 0.2 nM, n = 3. Inset, representative current traces from a single cell. a, control; b, 0.5 nM LqhαIT; c, 25 nM DRS + 0.5 nM LqhαIT. B, dose-response curve for the enhancement of LqhαIT effect induced by increasing concentrations of DRS with an EC₅₀ value of 56 ± 11 nM (n = 4). LqhαIT at 0.5 nM induces 8% inhibition of channel steady-state fast inactivation (see inset and the ●*). Inset, traces from a single cell used for the analysis of the dose response shown in Fig. 2B. C, inhibition of PbTx-2 effect by DRS. Alteration in conductance-voltage relations of DmNa_v1/TipE by PbTx-2 in the presence and absence of DRS. Toxin concentrations and the activation parameters (V_{1/2} in mV and k value, respectively) are: control, -15.9 ± 0.2 and 5.1 ± 0.2; PbTx-g (0.5 μM) -27.7 ± 0.3 and 7.3 ± 0.9; Drs (5 μM), -14.9 ± 0.6 and 5.3 ± 0.4; PbTx-2 + DRS (0.5 + 1 μM, respectively), -14.9 ± 0.9 and 5.5 ± 0.3. The data represent the mean ± S.E. of at least three independent experiments. Inset, DmNa_v1 currents from a single cell induced by a test pulse to -25 mV in the presence of control (a); 0.5 μM PbTx-2 + 1 μM DRS (b); 0.5 μM PbTx-2 (c).

in the fly hemolymph, shortly after an environmental stimulus, such as infection, DRS triggers a distinct response via interaction with DmNa_v1. Notably, *Drs* and *drs4* transcripts have been identified by microarray analysis in the *Drosophila* brain and thoracic-abdominal ganglia (FlyAtlas (21)). Moreover, *Drs* is highly transcribed in the BG2 cell line, which has originated from a *D. melanogaster* neuronal source (26; FLIGHT Database), suggesting that it might also be expressed next to its neuronal target. This observation suggests that DRS might act as a neuropeptide in the fly central nervous system. In this respect, it is interesting that some DRS homologues do not display any noticeable antifungal activity but are still transcribed (17) and therefore may possess other physiological roles. Interestingly, a study involving dozens of alleles of *Drs* and its homologues from several *Drosophila* species indicated that these loci were mostly subjected to purifying selection during their evolution, which resulted in strong conservation of the sequence of their peptide products (20). This may seem puzzling as many immune system related genes in insects are subjected to positive selection, which results in accelerated evolution and high sequence variability, thereby increasing the number of pathogen targets recognized and eliminated by the immune system (e.g. Ref. 27). Such unexpected conservation may be explained if DRS or some of its homologues also bind to a conserved target such as DmNa_v1. Overall, the ability of DRS, a major component of the *Drosophila* innate immune system, to bind and induce conformational alteration of the fly voltage-gated sodium channel is highly intriguing and paves new avenues in the study of the cellular targets and mode of action of peptides of this category. Additionally, this study raises questions regarding a possible interaction between the fly immune and nervous system.

REFERENCES

- Mouhat, S., Jouirou, B., Mosbah, A., De Waard, M., and Sabatier, J. M. (2004) *Biochem. J.* **378**, 717–726
- Froy, O., and Gurevitz, M. (1998) *FASEB J.* **12**, 1793–1796
- Zhu, S., Gao, B., and Tytgat, J. (2005) *Cell. Mol. Life. Sci.* **62**, 2257–2269
- Cohen, L., Karbat, I., Gilles, N., Froy, O., Corzo, G., Angelovici, R., Gordon, D., and Gurevitz, M. (2004) *J. Biol. Chem.* **279**, 8206–8211
- Karbat, I., Cohen, L., Gilles, N., Gordon, D., and Gurevitz, M. (2004) *FASEB J.* **18**, 683–689
- Karbat, I., Turkov, M., Cohen, L., Kahn, R., Gordon, D., Gurevitz, M., and Frolov, F. (2007) *J. Mol. Biol.* **366**, 586–601
- Cohen, L., Karbat, I., Gilles, N., Ilan, N., Benveniste, M., Gordon, D., and Gurevitz, M. (2005) *J. Biol. Chem.* **280**, 5045–5053
- Gurevitz, M., Karbat, I., Cohen, L., Ilan, N., Kahn, R., Turkov, M., Stankiewicz, M., Stühmer, W., Dong, K., and Gordon, D. (2007) *Toxicol.* **49**, 473–489
- Cohen, L., Lipstein, N., Karbat, I., Ilan, N., Gilles, N., Kahn, R., Gordon, D., and Gurevitz, M. (2008) *J. Biol. Chem.* **283**, 15169–15176
- Gordon, D., and Zlotkin, E. (1993) *FEBS Lett.* **315**, 125–128
- Poli, M. A., Mende, T. J., and Baden, D. G. (1986) *Mol. Pharmacol.* **30**, 129–135
- Landon, C., Sodano, P., Hetru, C., Hoffmann, J., and Ptak, M. (1997) *Protein Sci.* **6**, 1878–1884
- Moran, Y., Kahn, R., Cohen, L., Gur, M., Karbat, I., Gordon, D., and Gurevitz, M. (2007) *Biochem. J.* **406**, 41–48
- Zilberberg, N., Gordon, D., Pelhate, M., Adams, M. E., Norris, T. M., Zlotkin, E., and Gurevitz, M. (1996) *Biochemistry* **35**, 10215–10222
- Cohen, L., Lipstein, N., and Gordon, D. (2006) *FASEB J.* **20**, 1933–1935
- Shichor, I., Zlotkin, E., Ilan, N., Chikashvili, D., Stühmer, W., Gordon, D., and Lotan, I. (2002) *J. Neurosci.* **22**, 4364–4371
- Yang, W. Y., Wen, S. Y., Huang, Y. D., Ye, M. Q., Deng, X. J., Han, D., Xia, Q. Y., and Cao, Y. (2006) *Gene* **379**, 26–32
- Fehlbaum, P., Bulet, P., Michaut, L., Lagueux, M., Broekaert, W. F., Hetru, C., and Hoffmann, J. A. (1994) *J. Biol. Chem.* **269**, 33159–33163
- Hoffmann, J. A., Hetru, C., and Reichhart, J. M. (1993) *FEBS Lett.* **325**, 63–66
- Jiggins, F. M., and Kim, K. W. (2005) *Genetics* **171**, 1847–1859
- Chintapalli, V. R., Wang, J., and Dow, J. A. (2007) *Nat. Genet.* **39**, 715–720
- De Gregorio, E., Spellman, P. T., Rubin, G. M., and Lemaitre, B. (2001) *Proc. Natl. Acad. Sci. U.S.A.* **98**, 12590–12595
- Lemaitre, B., Reichhart, J. M., and Hoffmann, J. A. (1997) *Proc. Natl. Acad. Sci. U.S.A.* **94**, 14614–14619
- Hoffmann, J. A., and Reichhart, J. M. (2002) *Nat. Immunol.* **3**, 121–136
- Tzou, P., Reichhart, J. M., and Lemaitre, B. (2002) *Proc. Natl. Acad. Sci. U.S.A.* **99**, 2152–2157
- Takagi, Y., Ui-Tei, K., Miyake, T., and Hirohashi, S. (1998) *Neurosci. Lett.* **244**, 149–152
- Lazzaro, B. P. (2005) *Genetics* **169**, 2023–2034